Supplemental Information

Materials and methods

1. Experimental design

In the present study, all the mice were randomly assigned to different experimental groups as described below. The timelines of the two different experiments are shown in the experimental diagrams.

1.1 *Experiment 1*

To explore the pathology of depression, CUS was used to mimic the major behavioral features of depression [1]. After 2 weeks of adaptive feeding, forty-two adult male C57BL/6J mice were randomly divided into a control group (n = 19) and a CUS group (n = 23). The control group mice were raised under normal conditions for 4 weeks without any intervention. The CUS group of mice were subjected to different types of stressors for four successive weeks. The behavioral tests were performed 24 h after the last stress procedure.

1.2 *Experiment 2*

To verify the role of the hippocampal adiponectin/AdipoR1 pathway in the development of depressive-like behaviors and synaptic plasticity, hippocampal AdipoR1 was knocked down via the stereotactic injection of an AAV into the bilateral hippocampi of otherwise healthy mice. After adaptive feeding, twenty-six adult male C57BL/6J mice were randomly assigned to an AAV-normal control (AAV-Control) group (n = 13) and an AAV-AdipoR1 knockdown (AAV-AdipoR1-KD) group (n = 13). The mice in the AAV-control group were injected with AAV-U6-shRNA-CMV-EGFP (siRNA:TTCTCCGAACGTGTCACGTAA, titer 1.32×10^{13} vg/mL), and the mice in the AAV-AdipoR1-KD group were injected with AAV-U6-shRNA-AdipoR1-CMV-EGFP (siRNA:GGGACTGCTGTGTGTGTGTTGTA, titer 8.16×10^{12} vg/mL). The AAV was purchased from Hanbio Biotechnology Co., Ltd. (Shanghai, China). The behavioral tests were performed 4 weeks after virus injection.

2. CUS procedure

CUS was performed as described in previous experiments with some modifications [2] (Supplementary Table 1). The stressors included 24 h of food deprivation, 24 h of water deprivation, reversal of the light/dark cycle (lights off for 12 h during daylight hours and lights on for 12 h overnight), tilting the cage to 45°C overnight, strobe light exposure for 4 h, electric shock for 5 min (2.5 mA), shaking stress for 4 h (180 rpm), providing wet bedding overnight, light exposure overnight, and 4 h of restraint.

3. Stereotactic injection of AAV

The mice were anesthetized with isoflurane and fixed to a stereotaxic apparatus. The AAVs were injected bilaterally into the hippocampus (bregma, midlateral - 2.3 mm; anteroposterior ± 1.8 mm; dorsoventral -2.0 mm) at a slow rate (50 nl/min, 2 μl) with a syringe. After injection, the mice were placed on a heating pad until they recovered from the anesthesia.

4. Body weight measurement

The body weight reflects the growth status of the mice. The body weights of the mice in each group were measured regularly.

All subsequent experiments, including the analyses of behavior test, tissue preparation, Enzyme-linked immunosorbent assays, Western blot, Quantitative RT – PCR, Immunohistochemistry and immunofluorescence, Stereological analysis, et al., all the experiments and data analysis were performed blind to treatment conditions.

5. Behavioral assessments

5.1 Sucrose preference test (SPT)

The SPT was used to evaluate anhedonia in rodents [3] . All the mice were habituated to two bottles, one containing sucrose solution (1% (wt/vol)) and one containing drinking water, for 48 h of continuous exposure. To avoid a preference for the location of the bottles, their positions were switched after the first 24 h. During the SPT, the mice were allowed to interact with two bottles for

24 h, one containing sucrose solution (1% (wt/vol)) and one containing drinking water. The weights of the two bottles measured at the beginning and end of 24 h. Sucrose preference was calculated according to the following formula: sucrose preference (%) = sucrose consumption/(sucrose consumption + water consumption) ×100%.

5.2 Tail suspension test (TST)

The TST was used to measure “behavioral despair” [4]. Each mouse was suspended individually by its tail using adhesive tape to a tail suspension chamber under auditory and visual isolation conditions. The duration of the test was 6 min, and the immobility duration (%) within the final 4 min of testing was recorded.

5.3 Forced swimming test (FST)

The FST is a classic method used to evaluate stress-coping behavior in rodents [5] . The mice were individually placed in a transparent cylinder (diameter: 20 cm; height: 30 cm) filled with 15 cm of water (23 ± 1°C). The mice were monitored for 6 min via video tracking, and the immobility duration within the final 4 min of testing was recorded.

6. Tissue preparation

The mice were anesthetized intraperitoneally with sodium pentobarbital (40 mg/kg). Five mice randomly selected from each group were intracardially perfused with 10 ml of isotonic saline, followed by 40 ml of 4% paraformaldehyde (PFA). The brain tissues were isolated and postfixed in containers filled with 4% PFA. Five mice were randomly selected from the remaining mice, and blood samples from the retro-orbital venous plexus, the epididymis white adipose tissue (eWAT) and the bilateral hippocampal tissue of the mice were quickly collected and placed on ice. All the tissues were frozen in liquid nitrogen and stored at -80°C.

7. Enzyme-linked immunosorbent assays (ELISAs)

After anticoagulation, the blood samples were centrifuged at 4°C, and

plasma samples were collected. According to the manufacturer's protocol, ELISA kits were used to quantify the expression levels of total and high adiponectin in plasma (ALPCO^{TM} immunoassay, Cat # 80-ADPHU-E01, USA).

8. Western blot

Briefly, frozen hippocampal tissue was lysed with RIPA lysis buffer (Beyotime, China) containing 1% protease and phosphatase inhibitors (Beyotime, China) and homogenized on ice. The protein supernatants were collected after centrifugation, quantified with the bicinchoninic acid assay (Beyotime, China), mixed with 5x loading buffer (Beyotime, China) and deactivated at 95°C for 10 min. The proteins (20 mg) were separated with sodium dodecyl sulfate–polyacrylamide gel electrophoresis (SDS–PAGE) and transferred to polyvinylidene difluoride (PVDF) membranes (Thermo Fisher Scientific, USA). The membranes were blocked with blocking buffer (Beyotime), incubated with primary antibodies (rabbit anti-PSD95, CST, Cat #3450; mouse anti-microtubule-associated protein 2 (MAP2), Santa Cruz Biotechnology, sc-74421; rabbit anti-Synapsin-I a/b, Santa Cruz Biotechnology, sc-376623; rabbit anti-Gephyrin, Abcam, ab177154; rabbit anti-AdipoR1, Abcam, ab12661; mouse anti-AdipoR2, Santa Cruz Biotechnology, sc-514045; rabbit anti-HSP90, Abmart, T55548; and mouse anti-β-tubulin, Abmart, M30109F) and then immunoblotted with secondary antibodies matching the primary antibodies (anti-mouse IgG, Boster, BA1050; and anti-rabbit IgG, Boster, BA1054). The western blot images were visualized via an electrochemiluminescence system (Bio-Rad) and analyzed with ImageJ software (v.6.4).

9. Quantitative RT–PCR

Total RNA was extracted from eWAT and hippocampal tissue with TRIzol Reagent (Invitrogen). The RNA (500 ng) was reverse transcribed into cDNA with an Evo M-MLV RT Mix Kit with gDNA Clean for qPCR kits (Accurate Biology). The sequences of primers used for qPCR are listed in Table 2. Quantitative real-time PCR (RT–qPCR) was performed with a SYBR Green

Premix Pro Taq HS qPCR Kit (Accurate Biology). The RT–qPCR data were visualized with a CFX96 Real-time PCR Detection System (Bio-Rad). The expression of each gene was normalized to that of β-actin (Supplementary Table 2).

10. Immunohistochemistry and immunofluorescence

For immunohistochemistry, the brain tissues were equilibrated in a series of sucrose gradients for dehydration at 4°C (10%, 24 h; 20%, 24 h; and 30%, 48 h). One hemisphere was randomly selected for continuous sectioning into equal (50-μm-thick) sections after being embedded in optimal cutting temperature (OCT) compound. Every fifth tissue section was collected as a set of brain sections. One randomly selected set of brain sections was washed with 0.01 M PBS and permeabilization buffer (0.3% Tween-20 in PBS) for 30 min, immersed in blocking buffer containing 5% goat serum, 1% bovine serum albumin and 0.3% Tween-20 in PBS at 37°C for 2 h and then incubated with primary antibodies (rabbit anti-spinophilin, CST, Cat #14136) at 4°C for 72 h. The sections were then incubated with secondary antibodies (Electron Microscopy Sciences, ImmunoGold Reagents, goat anti-rabbit IgG) at 37°C for 3 h. Next, the sections were postfixed in the dark with 2% glutaraldehyde for 10 min. Subsequently, the sections were subjected to silver enhancement (Aurion R-Gent Silver Enhancement Kit, Electron Microscopy Sciences) at 25°C for 25 min and washed with deionized water followed by 0.01 M PBS. After being stained with hematoxylin for 1 min, the sections were dehydrated in gradient alcohol, cleared with xylene and sealed with neutral gum.

For immunofluorescence, the brain sections were equilibrated in a series of sucrose gradients for dehydration at 4°C (10%, 24 h; 20%, 24 h; and 30%, 48 h). One hemisphere was randomly selected for continuous sectioning into equal (30-μm-thick) sections after being embedded in OCT compound. Every fifth tissue section was collected as a set of brain slices. One randomly selected set of brain sections was washed with 0.01 M PBS and working buffer containing 0.3% Triton X-100 and 0.1% Tween-20 in PBS for 60 min. Then, the

sections were soaked in citrate solution for antigen repair in a water bath for 20 min, followed by incubation in blocking buffer (10% goat serum + 1% bovine serum albumin + 0.3% Tween-20 in PBS) at 37°C for 2 h. After blocking, the sections were incubated with primary antibodies (a mixture of primary anti-PSD95 and anti-MAP2 antibodies or a mixture of primary anti-Gephyrin and anti-MAP2 antibodies) at 4°C for 24 h. Then, the sections were incubated with secondary antibodies (DyLight 488-conjugated goat anti-rabbit IgG, DyLight 549-conjugated goat anti-mouse IgG, DyLight 549-conjugated goat anti-rabbit IgG, DyLight 649-conjugated goat anti-rabbit IgG, and Abbkine) at 37°C for 2 h, and the nuclei were stained with Hoechst-33342 (Sigma). Finally, the sections were pasted on glass slides. The fluorescent signals were visualized under a confocal laser microscope (FV3000, Olympus Corporation, Japan).

11. Stereological analysis

After immunohistochemical staining, the CA1, CA3 and DG regions were accurately traced and plotted under a light microscope at 4× magnification with a stereological system (Glostrup, Denmark). The spinophilin-immunoreactive puncta in the three regions of the hippocampus in each section were counted with the optical fractionator method under an oil objective lens at 100× magnification (N.A. 1.40). Optical fractionator counting was performed in the delineated regions of the sections in a systematic, random fashion so that each section had an equal probability of being sampled and that the intervals between sections and counting sites were constant. The total number of spinophilin^{+} spines (N) was estimated according to previous methods [6] .

An unbiased counting frame is shown in Supplementary Fig. 1A-1B. The solid line of the frame and its extension represent the exclusion lines, and the dotted line of the frame represents the inclusion line. When the inclusion (dotted) line turned green, the spinophilin-immunoreactive puncta that were completely inside the counting frame or partly inside the counting frame but

only touching the inclusion (dotted) line were counted.

12. Confocal laser analysis

The sections stained with anti-PSD95 or Gephyrin and anti-MAP2 antibodies were observed under a Nikon laser scanning confocal microscope (Nikon AIR, Nikon, Japan). The images were reconstructed in 3D to obtain the three-dimensional structure, and the number of synapses (labeled with anti-PSD95 or Gephyrin antibody) and the number of synapses on neurites (colabeled with anti-PSD95 or anti-Gephyrin and anti-MAP2 antibodies) in the hippocampus were counted with IMARIS software (Bitplane AG, Zurich, Switzerland). Image analysis was carried out with no postacquisition modifications. For the example images, brightness and contrast were adjusted within linear ranges with ImageJ/Fiji when necessary. The control and experimental conditions were adjusted with the same parameters.

13. Statistical analyses

Statistical analyses were carried out via SPSS (ver. 19.0, SPSS Inc., Chicago, USA), and the results are reported as the means ± standard deviations (SDs). All the data were assessed for normality and homogeneity of variance. The results of the BWT test were analyzed with repeated–measures ANOVA. The mean values between two groups were compared with the independent Student's t test for all the data, as they all conformed to a normal distribution in this study. Statistical significance was defined as a P value < 0.05.

Reference

1. Gupta D, Radhakrishnan M, Kurhe Y, Thangaraj D, Prabhakar V, Kanade P. Antidepressant-like effects of a novel 5-HT3 receptor antagonist 6z in acute and chronic murine models of depression. Acta Pharmacol Sin. 2014;35:1493–1503.
2. Antoniuk S, Bijata M, Ponimaskin E, Wlodarczyk J. Chronic unpredictable mild stress for modeling depression in rodents: Meta-analysis of model reliability. Neurosci Biobehav Rev. 2019;99:101–116.
3. Banasr M, Valentine GW, Li XY, Gourley SL, Taylor JR, Duman RS. Chronic unpredictable stress decreases cell proliferation in the cerebral cortex of the adult rat. Biol Psychiatry. 2007;62:496–504.
4. Steru L, Chermat R, Thierry B, Simon P. The tail suspension test: A new method for screening antidepressants in mice. Psychopharmacology (Berl). 1985;85:367–370.
5. Petit-Demouliere B, Chenu F, Bourin M. Forced swimming test in mice: a review of antidepressant activity. Psychopharmacology (Berl). 2005;177:245–255.
6. West MJ, Slomianka L, Gundersen HJG. Unbiased stereological estimation of the total number of neurons in the subdivisions of the rat hippocampus using the optical fractionator. Anat Rec. 1991;231:482–497.

Supplementary Figure Legend

Supplementary Fig. 1 Schematic of the unbiased counting frame. A: Schematic illustration of the optical dissector technique for counting spinophilin-immunoreactive puncta. The spinophilin-immunoreactive puncta that are clearly in focus in the guard zone, as indicated by the white arrow, were not counted. Scale bar = 40 μm. **B**: The spinophilin-immunoreactive puncta that are clearly in focus in the counting zone, as indicated by the white arrow, were counted. Scale bar = 40 μm.

Supplementary Fig. 2 CUS induced depressive-like behaviors in mice. A: Body weights of the mice. **B:** Immobility times in the FST of the mice. The data are shown as the means ± SDs. * indicates $P < 0.05$ between the CUS group and the Control group. ** indicates $P < 0.01$ between the CUS group and the Control group. *** indicates $P < 0.001$ between the CUS group and the Control group.

Supplementary Fig. 3 CUS induces a decrease in the number of dendritic spines in the three areas of the hippocampus. A: 3D schematic diagrams of immunofluorescence staining of MAP2 (red) and DAPI (blue) in the CA1, CA3 and DG regions of the Control group and CUS group. The area covered by the blue square represents the CA1 region, the area covered by the yellow square represents the CA3 region, and the area covered by the white square represents the DG region. Scale bar (two pictures on the top left and bottom left) = 500 μm. Scale bar (six pictures on the upper right and lower right) = 50 μm. **B:** Semiquantitative analyses of the intensity of MAP2 in the CA1, CA3 and DG regions of the Control group and CUS group. The data are shown as the means ± SDs. *** indicates $P < 0.001$ between the CUS group and the Control group.

Supplementary Fig. 4 CUS decreases the density of excitatory synapses in the three areas of the hippocampus. A: 3D schematic diagrams of immunofluorescence staining of PSD95 (green) and DAPI (blue) in the CA1, CA3 and DG regions of the Control group and CUS group. Scale bar = 50 μm. **B:** Semiquantitative analyses of the density of $PSD95^+$ synapses (PSD95-immunoreactive puncta) in the CA1, CA3 and DG regions of the Control group and CUS group. The data are shown as the means ± SDs. * indicates $P < 0.05$ between the CUS group and the Control group. ** indicates $P < 0.01$ between the CUS group and the Control group. *** indicates $P < 0.001$ between the CUS group and the Control group.

Supplementary Fig. 5 CUS decreases the density of inhibitory synapses in the three areas of the hippocampus. A: Representative western blot images of Gephyrin expression in the hippocampus. B: Gephyrin expression level in the hippocampus of the mice in the Control group and CUS group. C: 3D schematic diagrams of immunofluorescence staining of Gephyrin (green) and DAPI (blue) in the CA1, CA3 and DG regions of the Control group and CUS group. Scale bar = 50 μm. D: Semiquantitative analyses of the density of $Gephyrin^+$ synapses (Gephyrin-immunoreactive puncta) in the CA1, CA3 and DG of the Control group and the CUS group. The data are shown as the means ± SDs. * indicates $P < 0.05$ between the CUS group and the Control group. ** indicates $P < 0.01$ between the CUS group and the Control group. *** indicates $P < 0.001$ between the CUS group and the Control group.

Supplementary Fig. 6 Reductions in the expression of AdipoR1 in hippocampus induces depressive-behaviors. A: Body weights of the mice. **B:** Immobility times in the TST of the mice. The data are shown as the means ± SDs. * indicates $P < 0.05$ between the CUS group and the Control group. ** indicates $P < 0.01$ between the CUS group and the Control group. *** indicates $P < 0.001$ between the CUS group and the Control group.

Supplementary Fig. 7 Reductions in the expression of AdipoR1 in hippocampus induces a decrease in the number of dendritic spines in the three areas of the hippocampus. A: 3D schematic diagrams of immunofluorescence staining of MAP2 (red) and DAPI (blue) in the CA1, CA3 and DG regions of the Control group and AdipoR1KD group. The area covered by the blue square represents the CA1 region, the area covered by the yellow square represents the CA3 region, and the area covered by the white square represents the DG region. Scale bar (two pictures on the top left and bottom left) = 500 μm. Scale bar (six pictures on the upper right and lower right) = 50 μm. **B:** Semiquantitative analyses of the intensity of MAP2 in the CA1, CA3 and DG regions of the Control group and AdipoR1KD group. The data are shown as the means ± SDs. *** indicates $P < 0.001$ between the AdipoR1KD group and the Control group.

Supplementary Fig. 8 Reductions in the expression of AdipoR1 in hippocampus decreases the density of excitatory synapses in the three areas of the hippocampus. A: 3D schematic diagrams of immunofluorescence staining of PSD95 (green) and DAPI (blue) in the CA1, CA3 and DG regions of the Control group and AdipoR1KD group. Scale bar = 50 μm. **B:** Semiquantitative analyses of the density of $PSD95^+$ synapses (PSD95-immunoreactive puncta) in the CA1, CA3 and DG regions of the Control group and AdipoR1KD group. The data are shown as the means ± SDs. * indicates $P < 0.05$ between the AdipoR1KD group and the Control group. *** indicates $P < 0.001$ between the AdipoR1KD group and the Control group.

Supplementary Fig. 9 Reductions in the expression of AdipoR1 in hippocampus decreases the density of inhibitory synapses in three areas of the hippocampus. A: 3D schematic diagrams of

immunofluorescence staining of Gephyrin (green) and DAPI (blue) in the CA1, CA3 and DG regions of the Control group and AdipoR1KD. **B:** Semiquantitative analyses of the density of $Gephyrin^+$ synapses (Gephyrin-immunoreactive puncta) in the CA1, CA3 and DG regions of the Control group and the AdipoR1KD. Scale bar = 50 μm. The data are shown as the means ± SDs. * indicates $P < 0.05$ between the AdipoR1KD group and the Control group. ** indicates $P < 0.01$ between the AdipoR1KD group and the Control group. *** indicates $P < 0.001$ between the AdipoR1KD group and the Control group.

Supplementary Fig. 10 Hippocampal AdipoR1 expression was reduced in CUS model mice, and knockdown of AdipoR1 in the hippocampus of wild-type mic induced depression-like behaviors. Further results indicated that AdipoR1 deficiency led to significant synaptic deficits, mainly manifested as a reduced number of dendritic spines and a decreased density of excitatory/inhibitory synapses(PSD 95/Gephyrin) in hippocampal neurons.

Supplementary Fig. 1

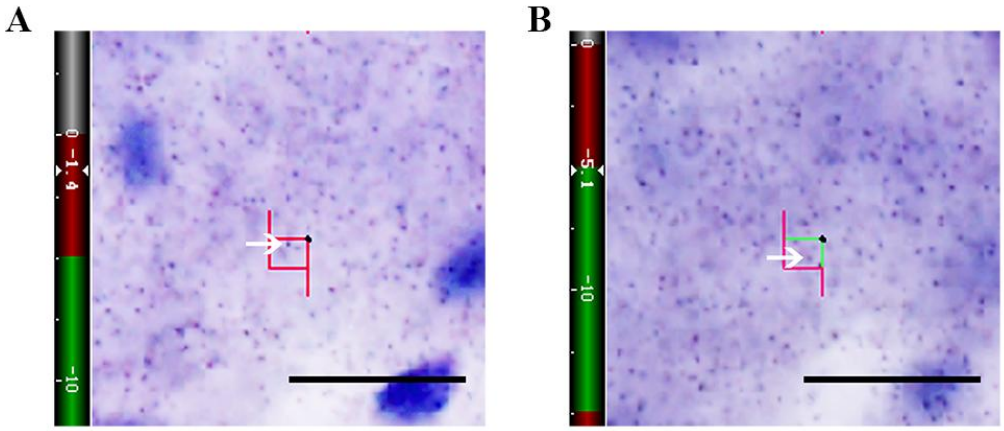

Supplementary Fig. 2

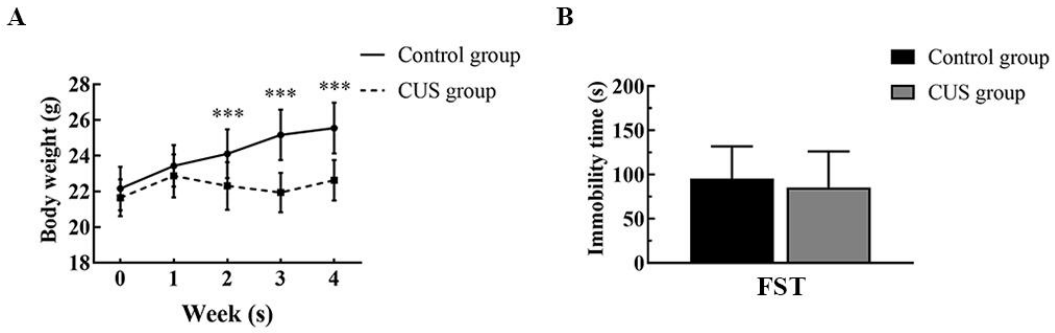

Supplementary Fig. 3

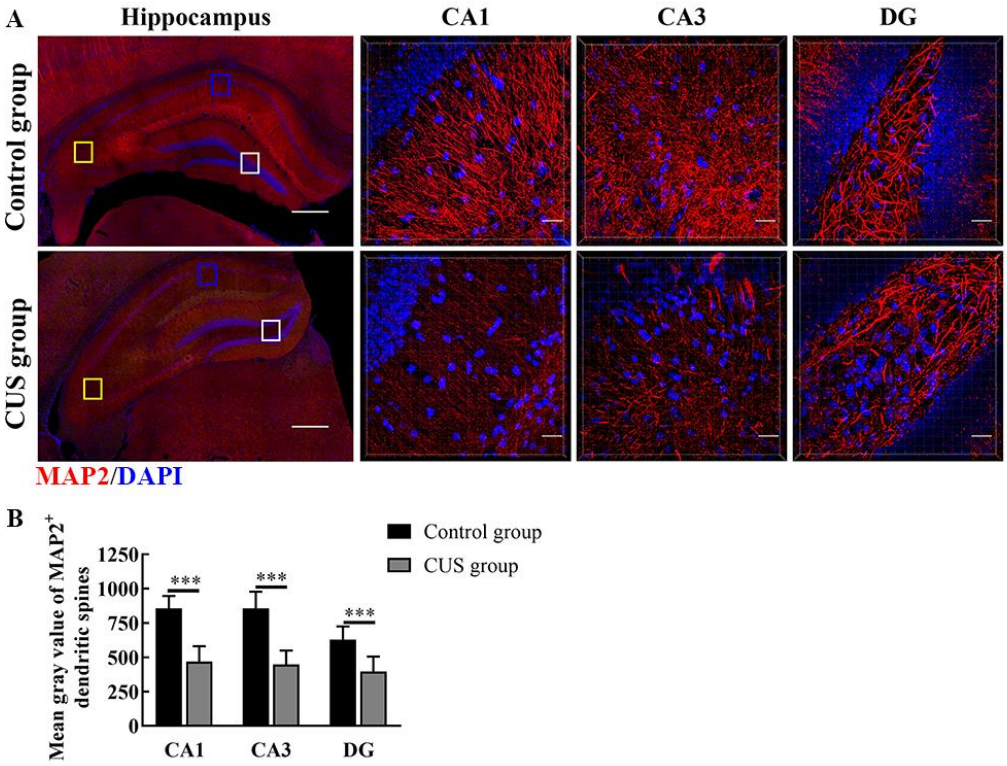

338 **Supplementary Fig. 4**

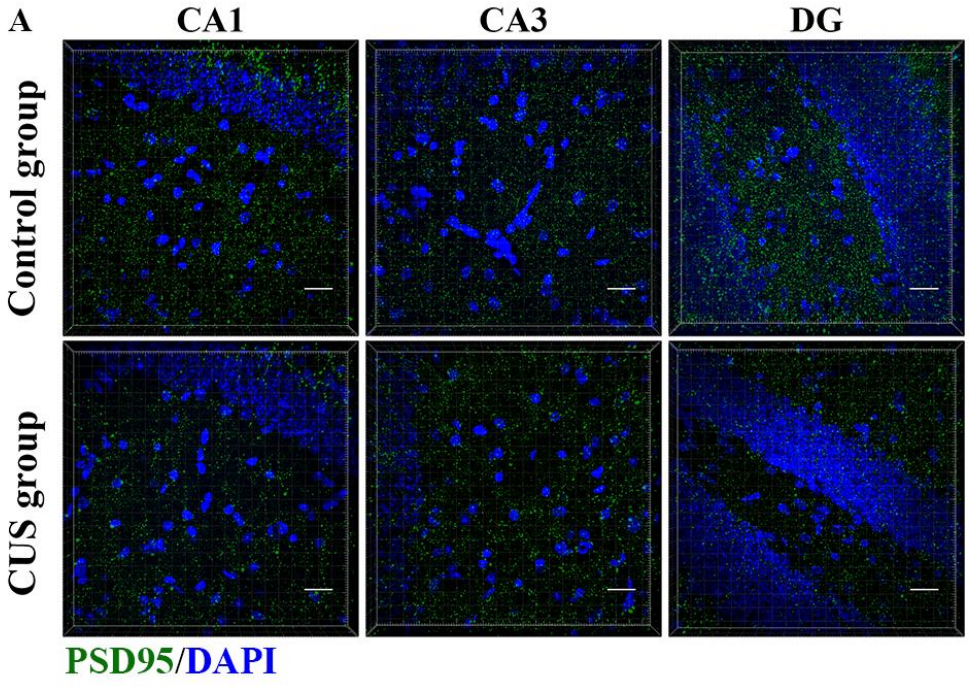

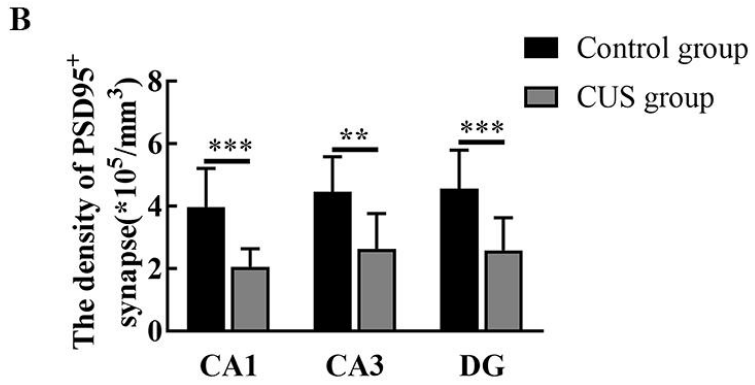

339
340

341 **Supplementary Fig. 5**

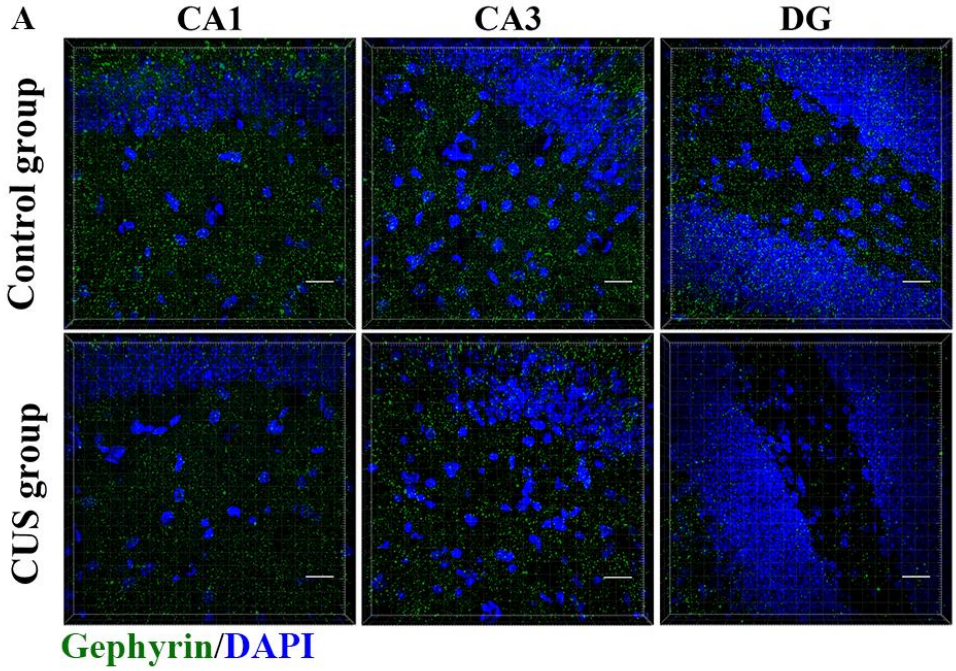

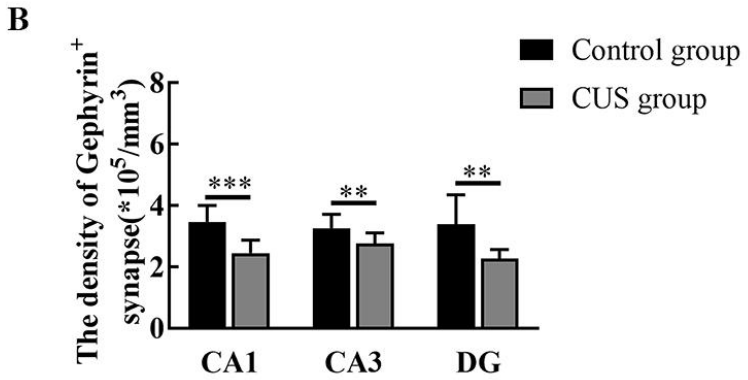

342
343

Supplementary Fig. 6

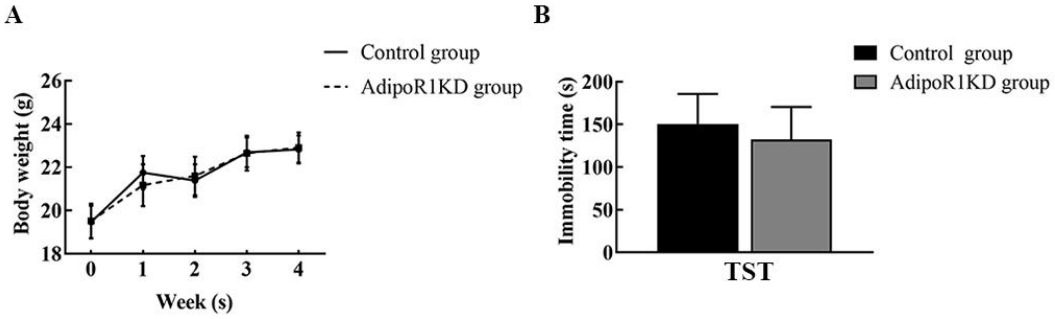

Supplementary Fig. 7

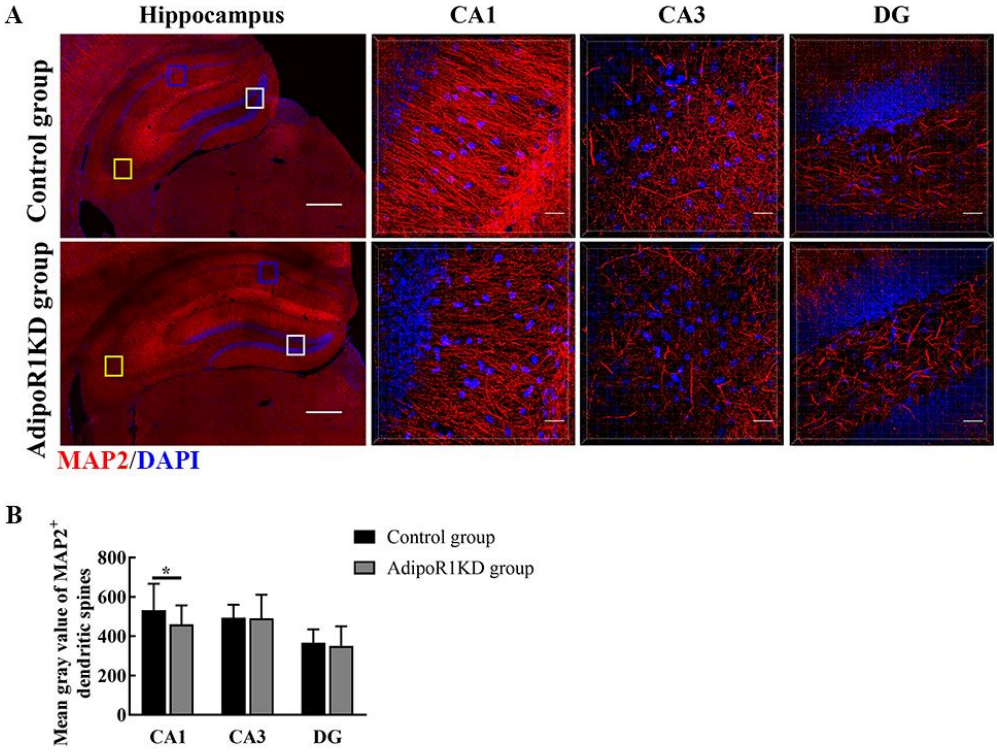

Supplementary Fig. 8

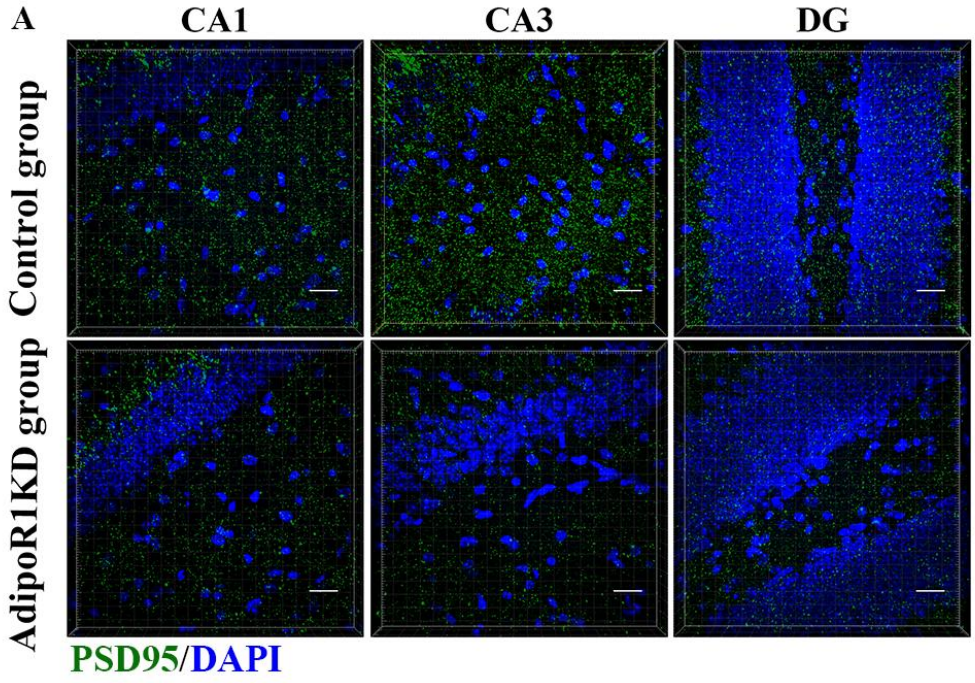

353 **Supplementary Fig. 9**

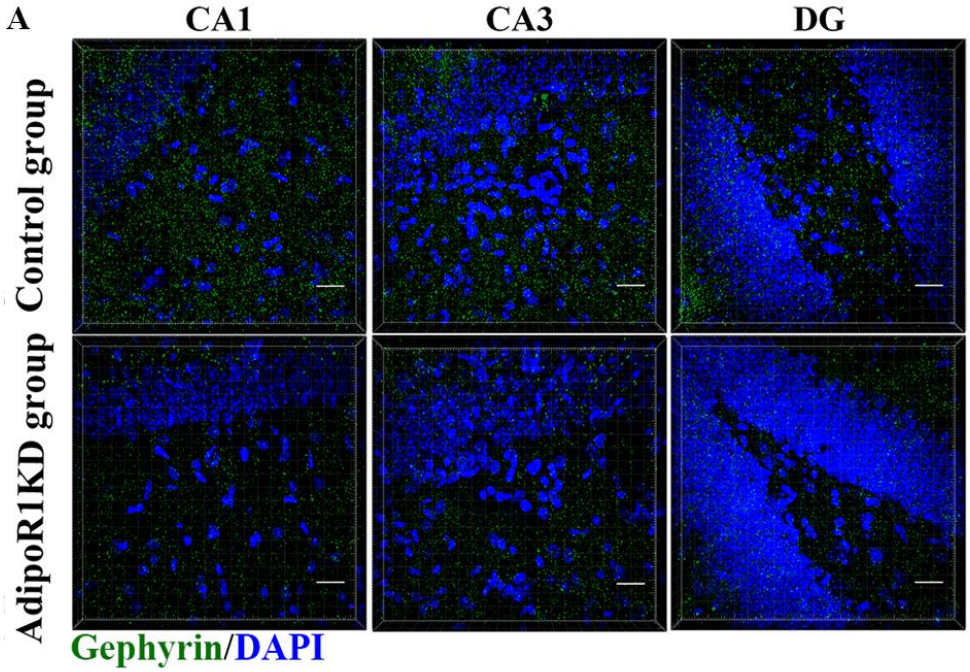

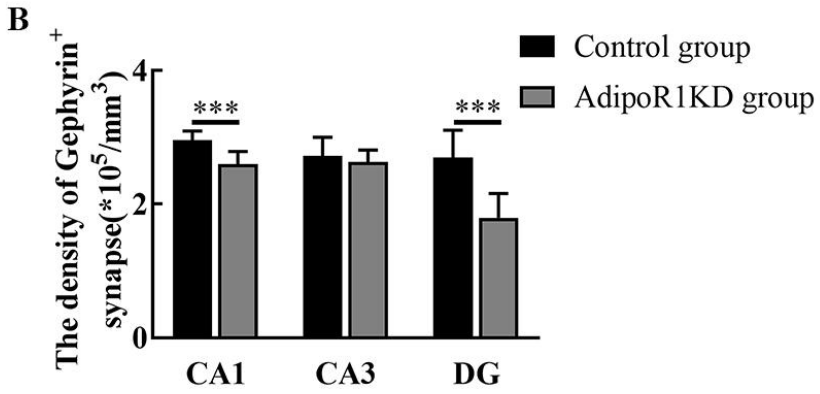

354
355

Supplementary Fig. 10

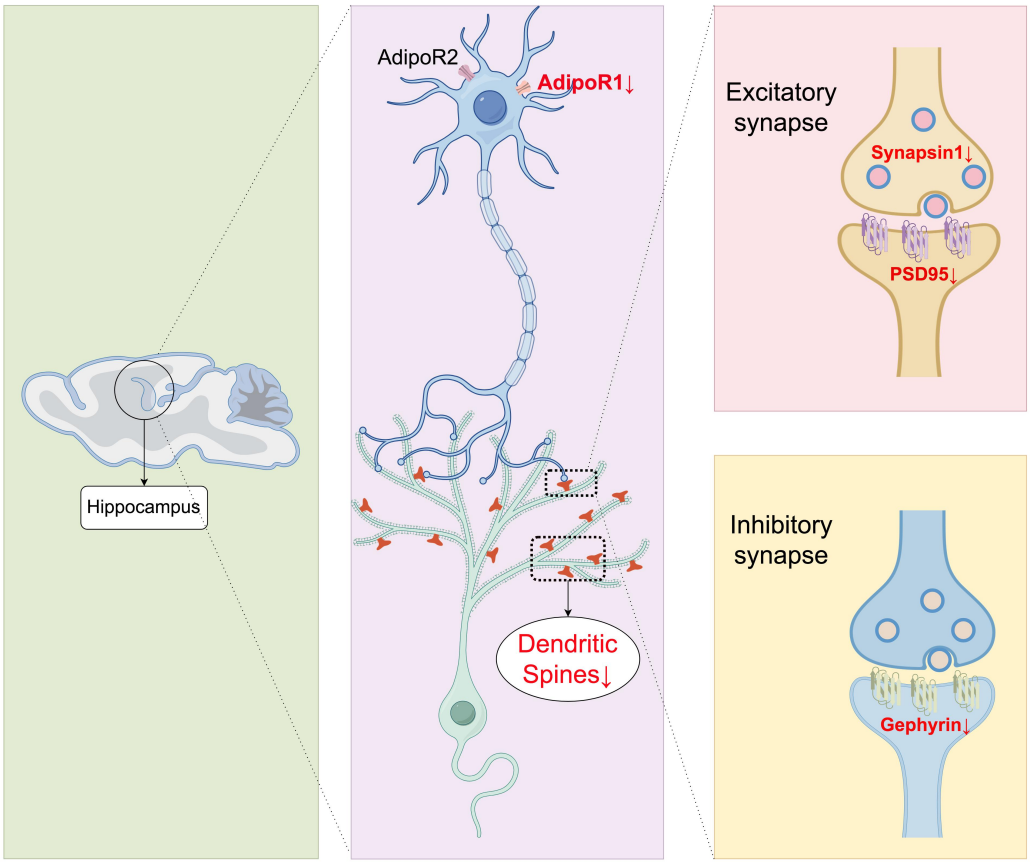

Supplementary Table Legend

Supplementary Table 1. Schedule of CUS stressor exposure.

Supplementary Table 2. Primer sequences for the quantitative real-time PCR assays

Supplementary Table 3. Statistics of all results in this study are provided

Supplementary Table 4. The details of target protein antibodies

Supplementary Table 1. Schedule of CUS stressor exposure.

Time	Monday	Tuesday	Wednes-day	Thursday	Friday	Saturday	Sunday
Week1	Electrical foot shock, Water deprivati-on	Empty bottle, Light off	Cold stress, Litter exchange	Table shaking, Cage tilting/ Empty bedding	Restrain, Food deprivati-on	BWT, Electrical foot shock, Exchange position; Strobe	Cold environm-ent, Changed bedding, Water deprivati-on
Week2	Empty bottle, Light off/on	Restraint, Food deprivati-on	Table shaking, Cage tilting/Em-pty bedding, Strobe lighting	Electrical foot shock, Strobe lighting	Table shaking, Exchange position; Litter exchange	BWT, Cold environm-ent, Restraint, Water deprivati-on	Change bedding, Water, Electrical foot shock, Empty bottle
Week3	Light off/on, Cold environm-ent, Table shaking	Electrical foot shock, Food deprivati-on, Cage tilting/Emp ty bedding	Table shaking, Restraint, Strobe lighting	Electrical foot shock, Wet bedding	Food deprivati-on	BWT, Empty bottle, Cold environm-ent, Light on	Electrical foot shock, Cage tilting/Em-pty bedding
Week4	Cold environm-ent, Table shaking, Light off/on	Electrical foot shock, Food deprivati-on, Cage tilting/Em-pty bedding	Table shaking, Restraint, Strobe lighting	Electrical foot shock, Wet bedding	Water deprivati-on	Empty bottle, Cold environm-ent, Light on	BWT, SPT, TST, FST

Supplementary Table 2. Primer sequences for the quantitative real-time PCR assays

Gene	Forward primers	Reverse primers	Length
β-Actin	ACGGTCAGGTCATCACTATCG	GGCATAGAGGTCTTTACGGATG	155
Adiponectin	CGACACCAAAAGGGCTCAGG	ACGTCATCTTCGGCATGACT	82
AdipoR1	CCTGGCTCTATTACTCCTTC	GAACACTCCTGCTCTTGTCT	149
AdipoR2	AGCCTCTATATCACCGGAGC	TTTGAGACTCCGTGGAAGTG	149

Sequences: 5’ to 3’.

373 **Supplementary Table 3** Statistics of all results in this study are provided

Fig.1		
Fig. 1B	Sucrose preference (Baseline)	$P = 0.589$ $t = 0.545 < t_{0.05, 41} = 2.021$
	Sucrose preference (After CUS)	$P < 0.001$ $t = 4.477 > t_{0.001, 41} = 3.551$
Fig. 1C	Immobility time in TST	$P < 0.05$ $t = 2.325 > t_{0.05, 41} = 2.021$
Fig. 1E	Protein levels of MAP2	$P < 0.01$ $t = 5.892 > t_{0.01, 4} = 4.604$
Fig. 1G	Protein expression levels of PSD95	$P < 0.05$ $t = 4.308 > t_{0.05, 4} = 2.776$
	Protein expression levels of Synapsin1	$P < 0.05$ $t = 4.454 > t_{0.05, 4} = 2.776$
Fig. 1I	Protein levels of Gephyrin	$P < 0.05$ $t = 3.910 > t_{0.05, 4} = 2.776$
Fig. 1N	Immunofluorescence intensity of $MAP2^+/PSD95^+$	CA1: $P < 0.001$ $t = 7.766 > t_{0.001, 46} = 3.551$
		CA3: $P < 0.001$ $t = 6.574 > t_{0.001, 46} = 3.551$
		DG: $P < 0.001$ $t = 7.889 > t_{0.001, 46} = 3.551$
Fig. 1O	Immunofluorescence intensity of $MAP2^+/Gephyrin^+$	CA1: $P < 0.001$ $t = 6.266 > t_{0.001, 22} = 3.792$
		CA3: $P < 0.001$ $t = 6.260 > t_{0.001, 22} = 3.792$
		DG: $P < 0.001$ $t = 6.309 > t_{0.001, 22} = 3.792$
Fig. 2		
Fig. 2A	The concentrations of total adiponectin in the plasma	$P < 0.01$ $t = 4.402 > t_{0.01, 6} = 3.707$
	The concentrations of HMW adiponectin in the plasma	$P < 0.05$ $t = 3.352 > t_{0.05, 6} = 2.447$
	The concentrations of MMW and LWM adiponectin in the plasma	$P < 0.01$ $t = 4.536 > t_{0.01, 6} = 3.707$
Fig. 2B	The adiponectin mRNA levels in eWAT	$P < 0.01$ $t = 5.460 > t_{0.01, 6} = 3.707$
Fig. 2C	mRNA levels of AdipoR1	$P < 0.05$ $t = 2.908 > t_{0.05, 4} = 2.776$

Fig. 2D	mRNA levels of AdipoR2	$P = 0.673$ $t = 0.460 < t_{0.05, 4} = 2.776$
Fig. 2F	Protein levels of AdipoR1	$P < 0.05$ $t = 3.807 > t_{0.05, 4} = 2.776$
Fig. 2H	Protein levels of AdipoR2	$P = 0.246$ $t = 1.358 < t_{0.05, 4} = 2.776$
Fig. 3		
Fig. 3C	Sucrose preference (Baseline)	$P = 0.922$ $t = 0.099 < t_{0.05, 24} = 2.064$
	Sucrose preference (After injection)	$P < 0.01$ $t = 3.583 > t_{0.01, 24} = 2.797$
Fig. 3D	Immobility time in FST	$P < 0.05$ $t = 2.474 > t_{0.05, 24} = 2.064$
Fig. 3E	mRNA levels of AdipoR1	$P < 0.05$ $t = 3.094 > t_{0.05, 4} = 2.776$
Fig. 3G	Protein levels of AdipoR1	$P < 0.001$ $t = 12.095 > t_{0.001, 4} = 8.610$
Fig. 3H	mRNA levels of AdipoR2	$P = 0.586$ $t = 0.592 < t_{0.05, 4} = 2.776$
Fig. 3J	Protein levels of AdipoR2	$P = 0.282$ $t = 1.446 < t_{0.05, 4} = 2.776$
Fig. 3K	The adiponectin mRNA levels in eWAT	$P = 0.772$ $t = 0.303 < t_{0.05, 6} = 2.447$
Fig. 3L	The concentrations of total adiponectin in the plasma	$P = 0.900$ $t = 0.131 < t_{0.05, 6} = 2.447$
	The concentrations of HMW adiponectin in the plasma	$P = 0.162$ $t = 1.596 < t_{0.05, 6} = 2.447$
	The concentrations of MMW and LWM adiponectin in the plasma	$P = 0.890$ $t = 0.145 < t_{0.05, 6} = 2.447$
Fig. 3M	The concentrations of total adiponectin in the CSF	$P = 0.434$ $t = 0.838 < t_{0.05, 6} = 2.447$
	The concentrations of HMW adiponectin in the CSF	$P = 0.142$ $t = 1.688 < t_{0.05, 6} = 2.447$
	The concentrations of MMW and LWM adiponectin in the CSF	$P = 0.627$ $t = 0.512 < t_{0.05, 6} = 2.447$
Fig. 4		
Fig. 4B	Number of spinophilin-immunoreactive	CA1: $P < 0.05$ $t = 2.647 > t_{0.05, 8} = 2.306$

	puncta	CA3: $P = 0.94$ $t = 1.897 < t_{0.05, 8} = 2.306$
		DG: $P < 0.05$ $t = 3.280 > t_{0.05, 8} = 2.306$
Fig. 4D	Protein levels of MAP2	$P < 0.05$ $t = 4.287 > t_{0.05, 4} = 2.776$
Fig. 4F	Protein expression levels of PSD95	$P < 0.05$ $t = 2.812 > t_{0.05, 4} = 2.776$
	Protein expression levels of Synapsin1	$P < 0.05$ $t = 2.873 > t_{0.05, 4} = 2.776$
Fig. 4H	Protein levels of Gephyrin	$P < 0.05$ $t = 2.873 > t_{0.05, 4} = 2.776$
Fig. 4M	Immunofluorescence intensity of $MAP2^+/PSD95^+$	CA1: $P < 0.001$ $t = 14.361 > t_{0.001, 46} = 3.551$
		CA3: $P < 0.001$ $t = 10.698 > t_{0.001, 46} = 3.551$
		DG: $P < 0.001$ $t = 5.899 > t_{0.001, 46} = 3.551$
Fig. 4N	Immunofluorescence intensity of $MAP2^+/Gephyrin^+$	CA1: $P < 0.001$ $t = 6.313 > t_{0.001, 22} = 3.792$
		CA3: $P < 0.001$ $t = 24.751 > t_{0.001, 22} = 3.792$
		DG: $P < 0.01$ $t = 3.671 > t_{0.01, 22} = 2.819$
Supplementary Fig. 2		
Supplementary Fig. 2A	Body wight (2^{nd} week)	$P < 0.001$
	Body wight (3^{rd} week)	$P < 0.001$
	Body wight (4^{th} week)	$P < 0.001$
Supplementary Fig. 2B	Immobility time in FST	$P = 0.404$ $t = 0.844 < t_{0.05, 41} = 2.021$
Supplementary Fig. 3		
Supplementary Fig. 3B	Immunofluorescence intensity of MAP2	CA1: $P < 0.001$ $t = 14.316 > t_{0.001, 54} = 3.496$
		CA3: $P < 0.001$ $t = 13.419 > t_{0.001, 54} = 3.496$
		DG: $P < 0.001$ $t = 8.342 > t_{0.001, 54} = 3.496$
Supplementary Fig. 4		

Supplementary Fig. 4B	Immunofluorescence intensity of PSD95	CA1: $P < 0.001$ $t = 6.876 > t_{0.001, 46} = 3.551$
		CA3: $P < 0.001$ $t = 5.616 > t_{0.001, 46} = 3.551$
		DG: $P < 0.001$ $t = 5.978 > t_{0.001, 46} = 3.551$
Supplementary Fig. 5		
Supplementary Fig. 5B	Immunofluorescence intensity of Gephyrin	CA1: $P < 0.001$ $t = 5.185 > t_{0.001, 22} = 3.792$
		CA3: $P < 0.01$ $t = 3.114 > t_{0.01, 22} = 2.819$
		DG: $P < 0.01$ $t = 3.869 > t_{0.01, 22} = 2.819$
Supplementary Fig. 6		
Supplementary Fig. 6A	Body wight (1st week)	$P = 0.107$
	Body wight (2nd week)	$P = 0.514$
	Body wight (3rd week)	$P = 0.877$
	Body wight (4th week)	$P = 0.751$
Supplementary Fig. 6B	Immobility time in TST	$P = 0.216$ $t = 1.271 < t_{0.05, 24} = 2.064$
Supplementary Fig. 7		
Supplementary Fig. 7B	Immunofluorescence intensity of MAP2	CA1: $P < 0.05$ $t = 2.101 > t_{0.05, 48} = 2.021$
		CA3: $P = 0.663$ $t = 0.430 < t_{0.05, 48} = 2.021$
		DG: $P = 0.465$ $t = 0.737 < t_{0.05, 48} = 2.021$
Supplementary Fig. 8		
Supplementary Fig. 8B	Immunofluorescence intensity of PSD95	CA1: $P < 0.001$ $t = 11.047 > t_{0.001, 46} = 3.551$
		CA3: $P < 0.001$ $t = 8.596 > t_{0.001, 46} = 3.551$
		DG: $P < 0.001$ $t = 4.904 > t_{0.001, 46} = 3.551$
Supplementary Fig. 9		

Supplementary Fig. 9B	Immunofluorescence intensity of Gephyrin	CA1: $P < 0.001$ $t = 5.293 > t_{0.001, 22} = 3.792$
		CA3: $P = 0.348$ $t = 0.959 < t_{0.05, 22} = 2.074$
		DG: $P < 0.001$ $t = 5.746 > t_{0.001, 22} = 3.792$

374

375 **Supplementary Table 4** The details of target protein antibodies

Antibodies	Species	Species	Catalog#	Dilution
Anti-MAP2 antibody	Mouse	Santa Cruz Biotechnology	SC-74421	1:1000
Anti-SynapsinI a/b antibody	Rabbit	Santa Cruz Biotechnology	SC-376623	1:500
Anti-PSD95 antibody	Rabbit	Cell Signaling Technology	Cat # 3450	1:500
Anti-PSD95 antibody	Rabbit	Cell Signaling Technology	Cat # 3450	1:500
Anti-Gephyrin antibody	Rabbit	Abcam	ab177154	1:200
Anti-AdipoR1 antibody	Rabbit	Novus Biological	NBP2-67631	1:1000
Anti-AdipoR2 antibody	Rabbit	ProteinTech	14361-1-AP	1:1000
Anti-Spinophilin antibody	Rabbit	Cell Signaling Technology	Cat # 14136	1:1000
Anti-β-tubulin antibody	Mouse	Abmart	M30109F	1:5000
Anti-HSP90 antibody	Rabbit	Abmart	T55548	1:5000
HRP anti-rabbit IgG	Goat	Boster	BA1054	1:5000
HRP anti-mouse IgG	Goat	Boster	BA1050	1:5000

376